The Journal of Experimental Biology 209, 2979-2989
Published by The Company of Biologists 2006
doi:10.1242/jeb.02314

Cloning and functional expression of voltage-gated ion channel subunits from cnidocytes of the Portuguese Man O'War *Physalia physalis*

C. Bouchard[1], R. B. Price[1], C. G. Moneypenny[1], L. F. Thompson[1], M. Zillhardt[1], L. Stalheim[1] and P. A. V. Anderson[1,2,*]

[1]*Whitney Laboratory for Marine Bioscience and* [2]*Department of Physiology and Functional Genomics, University of Florida, 9505 Ocean Shore Blvd, St Augustine, FL 32080, USA*

*Author for correspondence (e-mail: paa@whitney.ufl.edu)

Accepted 8 May 2006

Summary

Cnidocytes were dissociated from the tentacles of the Portuguese Man O'War *Physalia physalis* using heat treatment, and purified using density centrifugation. Visual observation confirmed that these cnidocytes contained a nucleus, a cnidocyst and an apical stereocilium, confirming that the cells were intact. A cnidocyte-specific amplified cDNA library was then prepared using RNA isolated from the cnidocytes, and screened for voltage-gated ion channel subunits using conventional molecular cloning techniques. A variety of channel proteins were identified and full-length sequence obtained for two of them, a Ca^{2+} channel β subunit (*Pp*Ca_Vβ) and a *Shaker*-like K^+ channel (*Pp*K_V1). The location of the transcripts was confirmed by RT-PCR of total RNA isolated from individually selected and rinsed cnidocytes. The functional properties of these two channel proteins were characterized electrophysiologically using heterologous expression. *Pp*Ca_Vβ modulates currents carried by both cnidarian and mammalian α_1 subunits although the specifics of the modulation differ. *Pp*K_V1 produces fast transient outward currents that have properties typical of other *Shaker* channels. The possible role of these channel proteins in the behavior of cnidocytes is discussed.

Key words: Ca^{2+} beta subunit, potassium channel, *Shaker*, K_V1, cnidaria, *Physalia physalis*.

Introduction

Cnidocytes, the defining character of members of the Phylum Cnidaria, are unique and enormously complex cells. Their most obvious feature is a single cnidocyst, a large membrane-enclosed organelle that occupies the bulk of the cell's volume. The cnidocyst consists of a hardened capsule, which encloses an inverted tubule. Discharge of the cnidocyst is thought to be an exocytotic event (for a review, see Kass-Simon and Scappaticci, Jr, 2002) whereby the cnidocyst membrane fuses with the apical end of the cnidocyte thereby exposing the capsule to the external medium. The elevated hydrostatic pressure inside the discharging cnidocyst then forces open the operculum on the apical end of the capsule and extrudes the inverted tubule out of the opening into (penetrants) or onto (adherents) the target.

Cnidocytes are used for a variety of functions, including food capture, locomotion and defense. Because of the complexity of the cell, and the fact that a cnidocyte can be used only once, their discharge is very tightly regulated to minimize what is likely to be the considerable energetic cost of replacement. Studies of the regulation of cnidocyte discharge have employed a variety of physiological (Gitter et al., 1994; Brinkmann et al., 1995; Purcell and Anderson, 1995; Salleo et al., 1996), structural (Lubbock et al., 1981; Westfall and Grimmelikhuijzen, 1993; Westfall, 2004) and histochemical approaches (Anderson et al., 2004; Kass-Simon and Scappaticci, Jr, 2004), using representatives of all cnidarian classes. Given that cnidocyte discharge is thought to be an exocytotic event, special attention (Lubbock et al., 1981; Gitter and Thurm, 1993; Gitter et al., 1994) has been given to the potential role of voltage-gated ionic currents, particularly Ca^{2+} currents of the type that trigger exocytosis at synapses and exocrine cells (Sudhof, 2004).

Voltage clamp recordings from single cnidocytes isolated from *Cladonema* (Class Hydrozoa) and *Chrysaora* (Class Scyphozoa) (Anderson and McKay, 1987) provided evidence for a variety of voltage-gated ionic currents in these cells. Stenotele cnidocytes from *Cladonema* are capable of producing a Na^+-dependent action potential and both they, and cnidocytes from *Chrysaora*, produce voltage-dependent K^+ currents. No evidence for voltage-gated Ca^{2+} currents was observed in either type of cnidocyte and in no instance did manipulation of a cell's membrane potential trigger cnidocyte discharge. Intracellular, current clamp recordings from

cnidocytes in the tentacles of *Physalia* (Anderson and McKay, 1987) provided no evidence for voltage-gated inward currents and again, cnidocyte discharge was never triggered by imposed changes in membrane potential.

Cnidocyte discharge does not, however, occur in Ca^{2+}-free media (Gitter et al., 1994), nor in the presence of inorganic Ca^{2+} channel blockers (Gitter and Thurm, 1993), suggesting that discharge is Ca^{2+}-dependent. Furthermore, because electrically induced discharge of *Hydra* cnidocytes is abolished in the absence of external Ca^{2+} (Gitter et al., 1994), it has been proposed that voltage-gated Ca^{2+} channels at the apical end of the cnidocyte are involved. However, although neurons are not always required for cnidocyte discharge (Aerne et al., 1991), cnidocytes are innervated by peptidergic (Anderson et al., 2004) and other classes of neuron (Kass-Simon and Scappaticci, Jr, 2004). Consequently, the effects of Ca^{2+}-free media and Ca^{2+} channel blockers could be manifest through their block of synaptic activity within the nerve nets that surround cnidocytes (Anderson et al., 2004; Price and Anderson, 2006), or at the level of synapses onto the cnidocytes themselves.

To resolve whether or not Ca^{2+} channels are present in cnidocytes, we employed molecular techniques to clone and localize voltage-gated Ca^{2+} channel subunits from a cnidocyte-specific amplified cDNA library. The results indicate that cnidocytes possess a variety of ion channels, including a Ca^{2+} channel α_1 and β subunit, and a voltage-gated K^+ channel. The Ca^{2+} β subunit is capable of modulating the activity of a mammalian and a cnidarian α_1 subunit, in a predictable manner, and the K^+ channel gates transient outward currents. While the presence of voltage-gated Ca^{2+} channel proteins in cnidocytes could reflect their role in the exocytosis that underlies cnidocyte discharge, other roles cannot be excluded.

Materials and methods

Cnidocyte purification

Fishing tentacles from newly captured *Physalia physalis* L. were placed in Ca^{2+}- and Mg^{2+}-free seawater, consisting of (mmol l^{-1}) NaCl, 450; KCl, 10; Na_2SO_4, 7; Hepes, 10 (pH 8.0). Pieces of the more distal, cnidocyte-rich ends of tentacles were transferred to pre-warmed (45°C) 500 μl, thin-walled polymerase chain reaction (PCR) tubes containing 250 μl of Ca^{2+}/Mg^{2+}-free artificial seawater (ASW). The final volume of tentacle in each tube was approximately 250 μl. The tubes were then maintained at 45°C for 15 min using an MJ Research MiniCycler PCR machine (Watertown, MA, USA), vortexed for 5 s, plunged into an ice bath for 30 s and the residual fragments of tentacle removed using fine forceps. The remaining liquid, which typically had a light blue tint, was then layered on chilled (4°C) Percoll (Sigma, St Louis, MO, USA) diluted 1:1.5 with concentrated ASW (McKay and Anderson, 1988) consisting of (mmol l^{-1}) NaCl, 1120; KCl, 22; $CaCl_2$, 20; $MgCl_2$, 65; $NaHCO_3$, 2. The samples were then spun at 5000 r.p.m. (2987 ***g***) in a Sorval RC 5B centrifuge for 15 min at 4°C, with the brake off. The aqueous layer at the top, together with the Percoll, was then removed with a pipette, and the pellet, which typically had a light blue appearance, was rinsed three times with Ca^{2+}/Mg^{2+}-free ASW.

The quality of the cnidocyte purification was assessed visually. A drop of resuspended pellet was placed on a 'Probe-on Plus' slide (Fisher Scientific, Suwanee, GA, USA) and left in a humid chamber for 30 min. 4% phosphate-buffered paraformaldehyde was then gently added and, after 30 min, replaced with fresh fixative. After a further 30 min, the sample was rinsed 3× for 10 min each with phosphate-buffered saline (PBS) that contained 0.25% Triton-X 100, stained with 0.008% 4′,6-diamidino-2-phenylindole (DAPI) in PBS for 20 min at room temperature, rinsed 3× for 10 min each in PBS and mounted in 90% glycerol in PBS.

RNA isolation and cDNA library production

RNA was prepared from the cnidocyte pellets or from intact tentacles, using published methods (Matz, 2002). Briefly, total RNA was isolated (Chomczynski and Sacchi, 1987), except that all procedures are performed at neutral rather than acidic pH. The RNA was precipitated with LiCl. Messenger RNAs were converted to cDNAs by reverse transcription with the TRSA primer, CGCAGTCGGTACTTTTTTTTTTT. A pseudo-double-stranded adaptor, made of two complementary oligonucleotides (CGACGTGGACTATCCATGAACGCAA-CTCTCCGACCTCTCACCGAGTACG and CGTACTCGGT), was then ligated to the 5′ end of the double-stranded cDNA. The structure of the adaptors evokes a PCR suppression effect which, through the process of self-annealing, prevents the amplification of molecules that have the adapter ligated to both ends (Lukyanov et al., 1997).

The library was then amplified using the primers CGACGTGGACTATCCATGAACGCA (DAP), which corresponds to part of the double-stranded adaptor, and TRSA, with the adapter ligation mix as the template. A smear was visible on a 1% agarose/ethidium bromide gel after 17 cycles of amplification.

Cloning of ion channel proteins

Fragments of ion channels were amplified from the cnidocyte cDNA library using degenerate oligonucleotide primers. In the case of the Ca^{2+} β subunit, these were AAYAAYGAYTGGTGGA (sense) and GCYTTYTGCAT-CATRT (anti-sense), which correspond to the conserved peptide sequences NNDWWI and DMMQK, respectively. For the K^+ channel, a sense primer (AAYGARTAYTTYGAYMG) corresponding to the peptide sequence NEYFFDR, and an anti-sense primer (CCRTAICCNASNGTIGTCAT) corresponding to the peptide sequence MTTVGYG, were used. The PCR reactions contained 50 pmol l^{-1} of each of the primers, 1 μl of the cDNA library, and LA Taq polymerase (Takara Mirus Bio, Madison, WI, USA). Thirty cycles of PCR amplification were carried out with a denaturing temperature of 94°C (1 min) and an extension temperature of 72°C (2.5 min). In the case of the Ca^{2+} β subunit the annealing temperature was 52°C (1 min). For the K^+ channel, a touchdown protocol from 60°C to 42°C

in 0.5°C increments was used. The products were run on agarose gels, and appropriately sized bands were excised, gel purified, ligated into the pGemT vector (Promega, Madison, WI, USA), and sequenced using the BigDye Terminator Cycle Sequencing Kit (ABI, Applied Biosystems Inc., Foster City, CA, USA). Full-length sequences for a Ca^{2+} β subunit and a K^+ channel were obtained with a RACE strategy using a combination of gene-specific primers and 5′- and 3′-adaptor-specific primers on the amplified cnidocyte library (Matz et al., 2003). The final sequence for each channel was derived from a consensus of three independent clones. Exact primers corresponding to the 5′ and 3′ end of this sequence were used to amplify a full-length cDNA from tentacle mRNA, which was sequenced to confirm its identity to the consensus.

To confirm the origin of the cloned ion channel subunits, 12 cnidocytes were removed from a suspension of purified cells by aspiration into a fine glass pipette whose tip diameter was slightly larger than that of cnidocytes. The isolated cnidocytes were transferred individually through three, 250 μl drops of Ca^{2+}/Mg^{2+}-free ASW on a glass coverslip. The continued presence of the divalent-free medium, coupled with the light mechanical agitation produced by the pipetting, should have minimized the possibility that fragments from other cells remained attached to the cnidocytes. Total RNA isolation and DNAase treatment were done using the Absolutely RNA Nanoprep kit (Stratagene, La Jolla, CA, USA). As much aqueous medium as possible was first removed from the drop on the slide, and replaced with cell lysis buffer. After cell lysis was observed, the entire volume of the drop was transferred to a microcentrifuge tube, and RNA isolation carried out according to the kit's instructions. In the case of the β subunit, PCR was performed on 2 μl of the reverse-transcribed product (Superscript III, Invitrogen, Carlsbad, CA, USA) using exact primers (GTTACAGCTTCGTACAATGTTCCTCT and CCA-TATTCTGAAGATGTACCAGAAGTT), which amplified a 323 bp region at the 5′ end of the coding sequence. Electrophoresis of the product on a 1% agarose gel revealed a band of the appropriate size that was then cloned and sequenced. For the K^+ channel, PCR with exact primers (CCAGCAAGCATCAGGGTTAT [sense] and ACTATAG-CCCACCACGATGC [antisense] produced a smear on the agarose gel after 30 cycles of amplification at an annealing temperature of 55°C. However, a further round of PCR with nested primers (CACGGGGCTTGCAGATCCTA [sense] and TGCCGCAGGTATAGAAGTAAATTTTG [antisense]) produced an intense band of the correct size after 20 cycles of amplification, using identical PCR conditions. This was cloned and sequenced.

Phylogenetic analysis

The phylogenetic relationship between the amino acid sequences of the cloned channel subunits and equivalent subunits in other organisms was determined using MrBayes3.1 (Ronquist and Huelsenbeck, 2003), a Bayesian phylogenetic inference program. The evolutionary model was based on a mixture of several fixed-rate amino acid models, and assumed gamma distribution of sites, according to variability. The analysis was run for 1.5 million generations, with a sample frequency of 100, concluding in a summary of the last 3000 trees (burnin=12,000). The analysis was run three times to ensure convergence. The graphical output was generated using Treeview (Page, 1996). All accession numbers refer to GenBank.

Heterologous expression

The functional properties of the cloned channels were determined as described previously (Jeziorski et al., 1999). In the case of the β subunit, this was done by co-expressing the transcript with cnidarian (*Cy*$Ca_V\alpha_1$; Accession number U93075) (Jeziorski et al., 1998) and mammalian ($Ca_V2.3$: Accession number NM009782) α_1 subunits. In the case of the K^+ channel, this was done by expressing the channel transcript directly. Briefly, stage V–VI oocytes removed from anesthetized adult female *Xenopus laevis* were defolliculated with the aid of 2 mg ml^{-1} collagenase (Sigma Type X) in Ca^{2+}-free ND96 solution consisting of (mmol l^{-1}): NaCl, 96; KCl, 2; $MgCl_2$, 1; Hepes, 5 (pH 7.4) and stored overnight at 17°C in ND96 with 1.8 mmol l^{-1} $CaCl_2$, supplemented with 2.5 mmol l^{-1} sodium pyruvate, 100 U ml^{-1} penicillin, 100 μg ml^{-1} streptomycin and 5% horse serum. For transcription, the full-length construct of the β subunit was ligated into an oocyte expression vector (Lingueglia et al., 1995), while that for the K^+ channel was transcribed directly from the pCR 4-TOPO cloning vector (Invitrogen). These were linearized using *Not*I and *Spe*I, respectively, purified with SDS and Proteinase K, followed by a phenol/chloroform extraction and precipitated with ethanol/sodium acetate. RNA was generated with an *in vitro* transcription reaction using the T7 version of the mMessagem Machine kit (Ambion Inc., Austin, TX, USA). The mRNA was purified and analyzed on a glyoxal denaturing gel. The β subunit mRNA was combined with either $Ca_V2.3$ or *Cy*$Ca_V\alpha_1$ in a 3:1 ratio to ensure an excess of the β subunit. For injections of either of the α_1 subunits alone, the mRNA was diluted 1:3 with water to ensure the same amount of message was injected. A total of 46 nl of mRNA was injected into each oocyte.

After 48 h of incubation at 17°C in supplemented ND96 medium, the properties of expressed currents were examined under two-electrode voltage clamp, as previously described (Jeziorski et al., 1999). Capacitive and leakage currents were removed using a P/3 routine. In recordings involving the β subunit, the actions of the endogenous Ca^{2+}-activated Cl^- currents in the oocytes were minimized by pre-treating the oocytes for 10 min in 0.5 mmol l^{-1} niflumic acid. The niflumic acid was prepared as a 250 mmol l^{-1} stock solution in ethanol and diluted 1:500 in recording solution. Ethanol alone at this concentration had no effect on the membrane potential or the current required to hold control oocytes at –90 mV.

Recordings were carried out using either ND96 (K^+ channel) or, in the case of the β subunit, a modified ND96 containing 40 mmol l^{-1} Sr^{2+} as the charge carrier (Jeziorski et al., 1998),

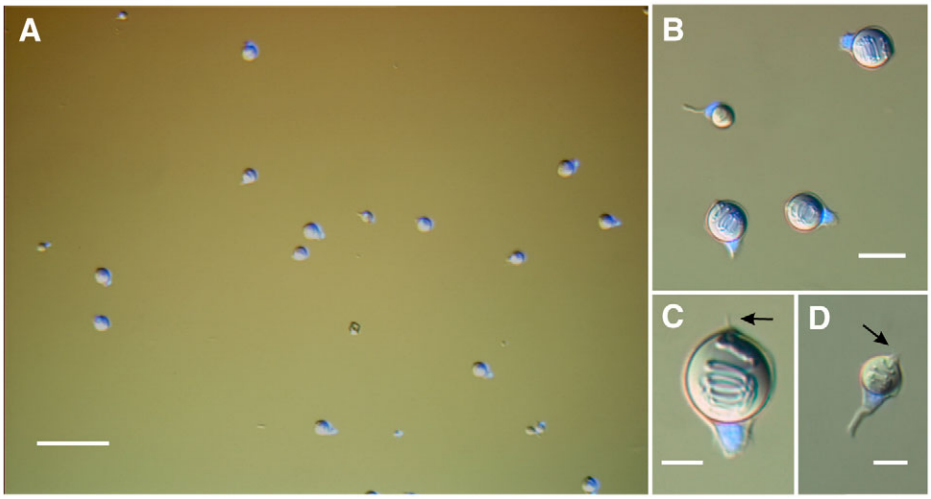

Fig. 1. Micrographs of cnidocytes isolated from the tentacles of *Physalia physalis.* (A) A low power micrograph showing the absence of other cell types. (B) A combined Normarski/fluorescence micrograph showing representatives of the two size classes of cnidocytes present in these preparations. Blue fluorescence of DAPI marks the nucleus of the cells. (C,D) Higher power Normarski/fluorescence micrographs of a single large (C) and small (D) cnidocyte. The DAPI-stained nucleus is very evident at the base of the cyst in each cell. The cnidocil at the apical end of each cell is marked with an arrow. Note the cytoplasmic projections at the base of the cells. Scale bars: 200 μm (A), 50 μm (B), 20 μm (C,D).

since both $Ca_V2.3$ and *Cy*$Ca_V\alpha_1$ show greatest selectivity for Sr^{2+}. Only oocytes with resting potentials of at least –20 mV and requiring holding currents of less than –0.20 μA when clamped at –90 mV were used in this study.

Results

The protocol used to isolate cnidocytes from the tentacles of *Physalia* yielded preparations of cells that were composed entirely of cnidocytes (Fig. 1A), together with the occasional cnidocysts, some of which had discharged. Single isolated nuclei were occasionally observed in DAPI-stained preparations, together with small amounts of cellular debris, but no other intact, recognizable cell types were ever observed.

The isolated cnidocytes fell into two size classes with, so far as could be determined from examination of the discharged and undischarged cysts, structurally similar cysts. In both instances, the cells contained a single, spherical cnidocyst, which occupied the bulk of the apical portion of the cell leaving very little space between the margin of the cyst and that of the cell. In the larger of the two, the cysts measured 40 μm in diameter. They occupied almost the entire volume of the cell, leaving only a small truncated conical projection at the basal end of the cell (Fig. 1B,C). This projection, which contained the nucleus, terminated in an array of fine processes that projected away from the cell body. A cnidocil was evident at the apical end of the cell but stereo-cilia were not obvious (Fig. 1C). In the smaller of the two classes of cnidocyte, the cnidocyst measured 22 μm in diameter and occupied a smaller proportion of the cell. A long narrow cytoplasmic projection extended from the basal end of these cells; the cell's nucleus lies in this process, basal to the cyst (Fig. 1D). These cells also bore a cnidocil which was less distinct than those of the larger cells, but appeared to be surrounded by a collar of sterocilia. The total length of both types of cnidocyte, from the apical end of the cell to the end of the basal cytoplasmic extension, were the same (55–60 μm), presumably representing the width of the tentacle ectoderm.

Ca^{2+} β subunit

The initial fragment of the *Physalia* Ca^{2+} channel β subunit was obtained using two degenerate oligonucleotide primers that correspond to conserved regions of mammalian β subunits. These have been used successfully to isolate β subunits from a flatworm (Kohn et al., 2002). The remainder of the *Physalia* β subunit, which we term *Cy*$Ca_V\beta$, was obtained using a RACE strategy. The 533-amino-acid polypeptide is encoded by a 1599-base-pair open reading frame and has a deduced molecular mass of 59 kDa. The sequence for this subunit has been submitted to GenBank (Accession number: ABD59026).

The primary sequence of *Pp*$Ca_V\beta$ is most similar (62% identity; 76% conserved) to that of *Cy*$Ca_V\beta$ from the scyphozoan jellyfish *Cyanea capillata,* but is generally similar to that of other β subunits (Fig. 2) particularly in the two regions that create the sides of the AID binding pocket (for a review, see Richards et al., 2004). Moreover, of the 17 residues that have been shown, through crystallization studies (Chen et al., 2004), to interact directly with the α_1 subunit in mammalian Ca^{2+} channels, all but two are identical in *Pp*$Ca_V\beta$ (Fig. 2), and one of those is conserved.

A phylogenetic tree showing the relationship of *Cy*$Ca_V\beta$ to a variety of other β subunits is presented in Fig. 3. This tree groups the two cnidarian β subunits together, distinctly separate from the two β subunits from the platyhelminth

Fig. 2. An alignment of the amino acid sequence of the *Physalia* β subunit *(Pp*$Ca_V\beta$*)* (GenBank Accession number: ABD59026) with β subunits from the scyphozoan jellyfish *Cyanea capillata* (*Cy*$Ca_V\beta$ [Accession Number: AAB87751]), one each from the platyhelminth *Schistosoma mansoni* (*Sm*$Ca_V\beta2$ [AAK51118]), *Drosophila* (*Dm*$Ca_V\beta$ [AAF21096]), rabbit ($Ca_V\beta1$ [P19517]) and human ($Ca_V\beta2$ [AAL73495]). Conservation (100%) is indicated by white letters on a black background and greater than 80% conservation by white letters on a gray background. Residues that interact directly with the AID domain of the α_1 subunit have a red background. This alignment was obtained using ClustalX (Version 1.83) and displayed using Genedoc (Vers. 2.6.002).

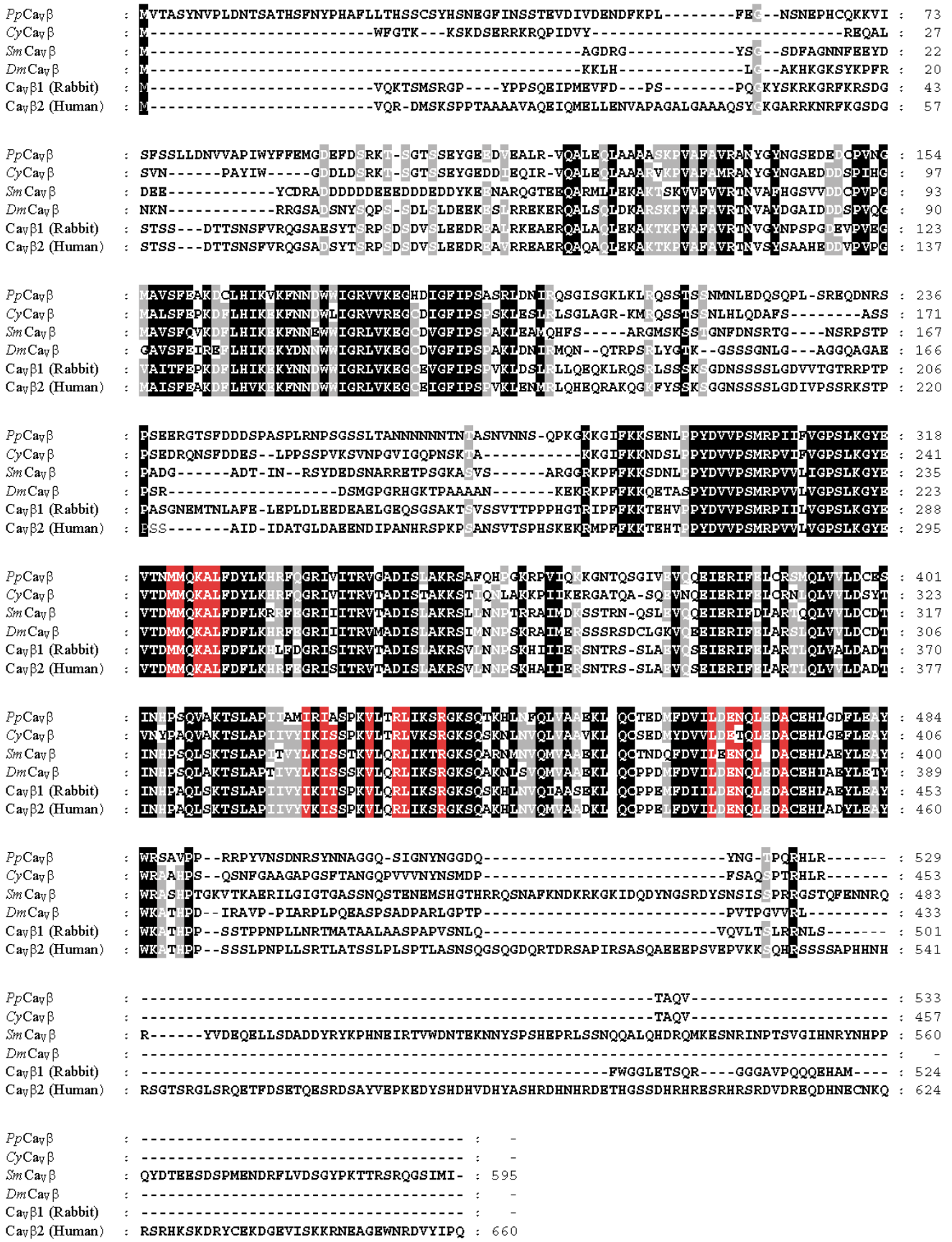

Fig. 2. For caption see previous page.

Schistosoma manson and distant from insect and mammalian β subunits.

Co-expression of *Pp*Ca_Vβ with *Cy*$Ca_V\alpha_1$ from the jellyfish *Cyanea* modulates the properties of currents gated by *Cy*$Ca_V\alpha_1$ alone. The most prominent effect is a threefold increase in the peak of current (Fig. 4A,B) through the channel. When currents with and without *Pp*Ca_Vβ are normalized and fit to a modified Boltzman equation, a negative shift in the *I/V* relationship is evident (Fig. 4D). Finally, inactivation of *Cy*$Ca_V\alpha_1$ is accelerated by *Pp*Ca_Vβ (Fig. 4F). In contrast, while co-expression of *Pp*Ca_Vβ with the mammalian $Ca_V2.3$ results in a twofold increase in the peak current (Fig. 4C), the shift in the *I/V* relationship of the normalized currents is less marked than that for *Cy*Ca_Va1 (Fig. 4E), and there is no obvious effect on the rate of inactivation (Fig. 4G).

Voltage-gated K⁺ channel

The use of degenerate K^+ channel primers and conventional cloning methods yielded a cDNA that encodes for a 481-amino-acid protein with high sequence homology to voltage-gated K^+ channels (Fig. 5). The 55 kDa protein bears an N-linked glycosylation site on the extracellular loop between transmembrane segments I and II, and a total of 16 consensus phosphorylation sites exposed on the cytoplasmic face of the protein. The sequence for this channel has been submitted to GenBank (Accession number: ABD59027). Phylogenetic analysis shows that it is most similar to the k_V1 (*Shaker*) family of voltage-gated K^+ channels (Fig. 6) and it clusters most closely to jShak1, a *Shaker*-like channel from the hydromedusa *Polyorchis*.

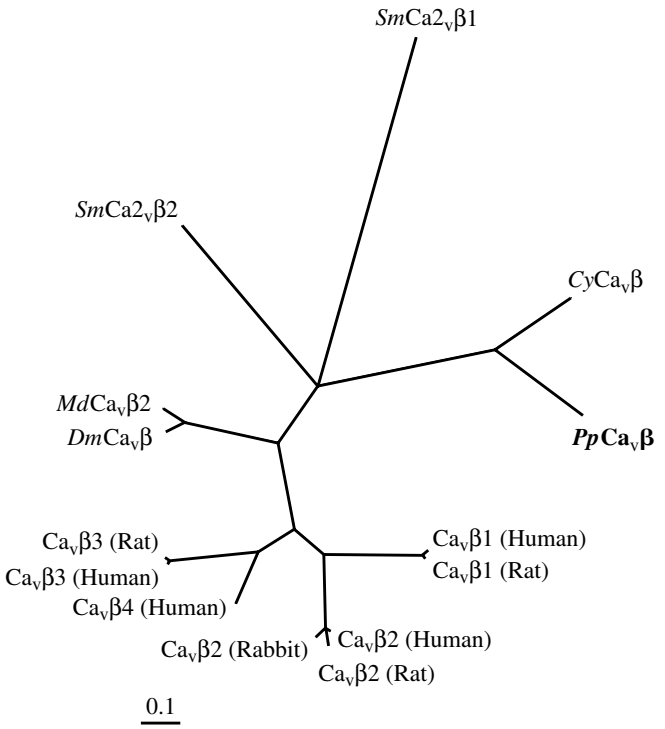

Fig. 3. An unrooted phylogenetic tree showing the relationship of *Pp*Ca_Vβ (shown in bold type) to other β-subunits. Subunits included in this alignment are *Cy*Ca_Vβ from the scyphozoan jellyfish *Cyanea capillata* [GenBank Accession number AAB87751], *Sm*Ca_Vβ1 [AAK51117] and *Sm*Ca_Vβ2 [AAK51118] from the platyhelminth *Schistosoma mansoni*, *Dm*Ca_Vβ [AAF21096] from *Drosophila,* *Md*Ca_Vβ [A54844] from the fly *Musca*, and eight members of vertebrate β subunits subfamilies found in rabbits (Ca_Vβ2 [P54288]); rat (Ca_Vβ1[P54283], Ca_Vβ2[Q8VGC3] and Ca_Vβ3[P54287]), and human (Ca_Vβ1 [Q02641], Ca_Vβ2 [AAL73495], Ca_Vβ3 [BAA07803], Ca_Vβ4 [O00305]). Only the bipartitions supported at greater than 95% probability are shown. Scale bar represents the average number of replacements per site.

Two-electrode voltage clamp recordings from *Xenopus* oocytes expressing *Pp*K_V1 revealed the presence of fast, transient outward currents (Fig. 7A) that activate around –30 mV (Fig. 7B). These currents activate rapidly and inactive with time constants as fast as 4 ms but they never fully inactivate, leaving a small steady state outward current. The voltage-dependency of inactivation of this channel was measured using prepulses to a range of potentials. 50% inactivation occurred around –18 mV (Fig. 7C). This current was blocked by extracellular 10 mmol l^{-1} 4-aminopyridine (4-AP) and 5 mmol l^{-1} tetraethyl ammonium (TEA) (data not shown).

A truncated version of this channel, which began at Met^{21} of the full-length sequence, expressed robustly (not shown) but instead of transient outward currents, this clone produced non-inactivating currents. These currents had the same activation potential as the full-length channel, were blocked by extracellular TEA, less so by 4-AP, and showed only slight voltage-dependent steady-state inactivation.

Attempts to confirm the location of these channel transcripts using *in situ* hybridization have not been successful to date. Instead, the cellular origin of *Pp*Ca_Vβ and *Pp*K_V1 mRNA was confirmed by RT-PCR directly from cnidocytes RNA, as described in the Materials and methods. Sequencing of the band obtained using *Pp*Ca_Vβ- or *Pp*K_V1-specific primers yielded identical sequences to the respective channels, thereby confirming that both *Pp*Ca_Vβ and *Pp*K_V1 are present in cnidocytes. In both cases, PCR performed under identical conditions but in the absence of template, yielded no product. Another control experiment consisted of an amplification, using both primer sets, of cDNA from the wall of the pneumatophore. Again, this yielded no product, whereas PCR of the same template with actin-specific primers produced the appropriate product.

Discussion

Cnidocytes are often considered to be among the most complex cells in biology. This characterization is quite justifiable given their very complex structure, development and unique function (for a review, see Kass-Simon and Scappaticci, Jr, 2002). One consequence of their complexity is that the cost of replacing cnidocytes, which can only be used once, is likely to be relatively high. Thus, it is perhaps not surprising that discharge of these cells is tightly

regulated so as to ensure that they are only used at the optimal time.

Work in the field of the regulation of cnidocyte discharge over the years has demonstrated that cnidocytes do not function as independent effectors, as originally surmised (Parker, 1916), but instead normally function in concert with a multicellular

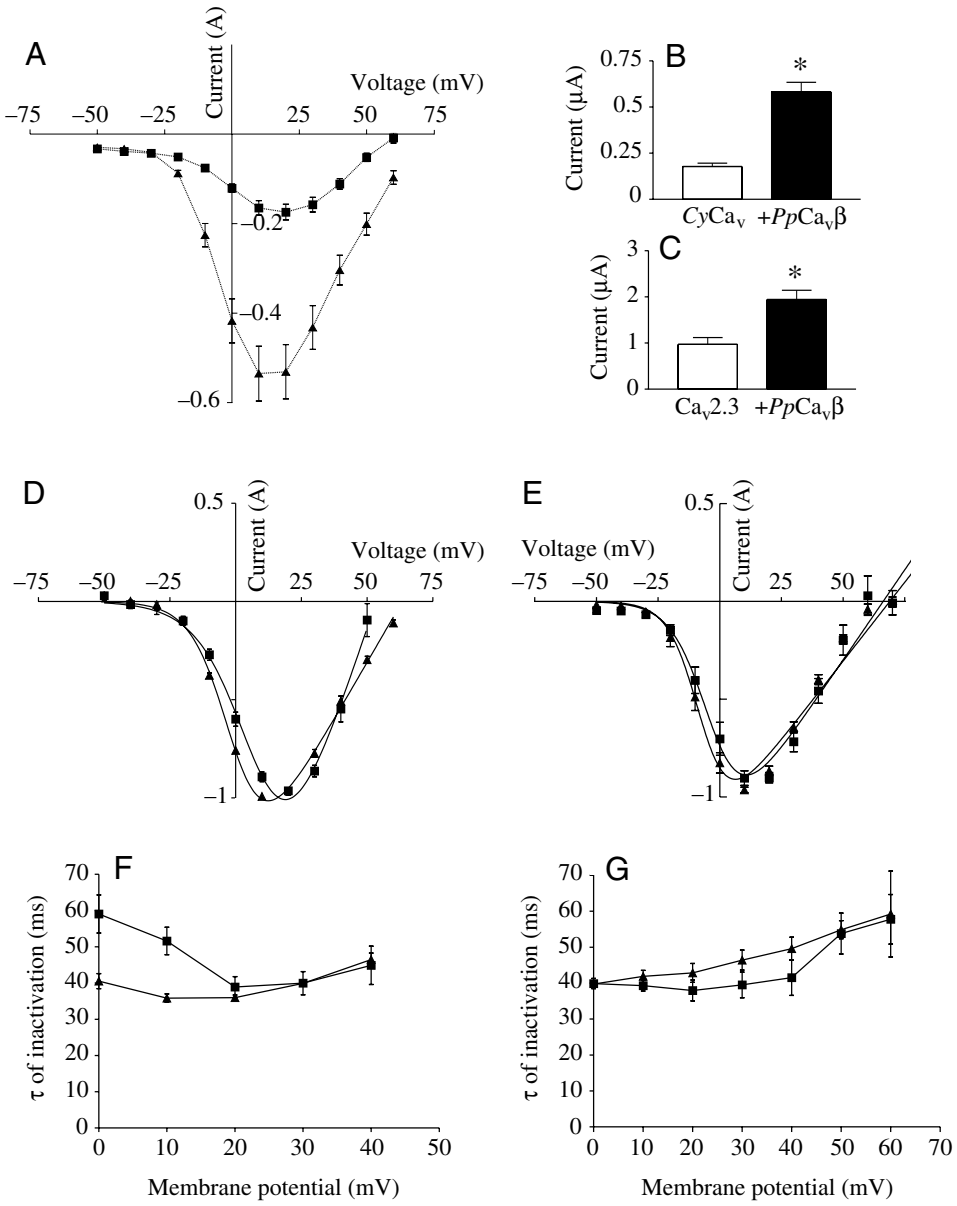

Fig. 4. Functional expression of *Pp*Ca$_V$β. (A) Current/voltage relationships of currents gated by *Cy*Ca$_V$ in the presence (triangles) and absence (squares) of *Pp*Ca$_V$β. Values are means ± s.d. of from 13 (triangles) to 16 (squares) trials. (B) Peak amplitude (± s.d.) of currents gated by *Cy*Ca$_V$ in the presence (black bar; N=13) and absence (white bar; N=16) of *Pp*Ca$_V$β. In the presence of *Pp*Ca$_V$β, currents are significantly larger ($P<2\times10^{-6}$). (C) Same, for currents gated by Ca$_V$2.3 in the presence (dark bar; N=14) and absence (white bar; N=14) of *Pp*Ca$_V$β. In the presence of *Pp*Ca$_V$β currents are significantly larger ($P<0.012$). (D) Current/voltage relationship of normalized currents (± s.d.) gated by *Cy*Ca$_V$ in the presence (triangles; N=13) and absence (squares; N=16) of *Pp*Ca$_V$β. Co-expression with *Pp*Ca$_V$β results in an obvious negative shift in the I/V relationship. (E) The same, for currents gated by Ca$_V$2.3 in the presence (triangles; N=16) and absence (squares; N=14) of *Pp*Ca$_V$β. The *I*/*V* relationship of Ca$_V$2.3 is altered slightly by co-expression with *Pp*Ca$_V$β. Data points in D and E are fitted by the Boltzman function $I_{norm}=g_{norm}(V-V_{rev})/(1+\exp[-(V-V_{1/2})]/k$, where g=conductance, V_{rev}=53.44, 63.4, 66.25 and 68.94, $V_{1/2}$=9.68, –0.5652, –3.067 and –7.281 and k=9.443, 7.152, 7.357, and 6.163 for *Cy*Ca$_V$, *Cy*Ca$_V$/*Pp*Ca$_V$β, Ca$_V$2.3 and Ca$_V$2.3/*Pp*Ca$_V$β. (F) The relationship between time constant of inactivation of currents in the presence (triangles; N=14) and absence (squares; N=9) of *Pp*Ca$_V$β. The time constant of inactivation was determined by fits of exponential curves to the decay phase of the current. At +10 mV, the time constant of inactivation of the current is significantly faster ($P>0.0015$) in the presence of *Pp*Ca$_V$β. (G) Same, for currents gated by Ca$_V$2.3. There was no significant difference in the rate of inactivation under the two conditions.

pathway composed of sensory cells (Holtmann and Thurm, 2001; Westfall, 2004), neurons (Kass-Simon and Scappaticci, Jr, 2004; Price and Anderson, 2006) and in some instances, supporting cells (Watson and Roberts, 1995). One consequence of the fact that multiple cell types are involved in the regulation of discharge has been the challenge of localizing the site of action of some experimental manipulations. For example, several studies have concluded that voltage-gated Ca^{2+} channels are involved in discharge (Lubbock et al., 1981; Gitter and Thurm, 1993; Gitter et al., 1994), and while it has been assumed that Ca^{2+} channels play a direct role on the exocytotic event underlying discharge, the possibility that those channels are present at synapses within the nerve nets that innervate cnidocytes cannot be excluded. Distinguishing between these possibilities is compounded by the small size and diffuse nature of many of the cells in question, particularly the neurons.

To circumvent this problem, we chose to take advantage of the elevated density of cnidocytes to create a cnidocyte-specific cDNA library, and to screen that library for genes that encode for likely components of any regulatory pathways. A variety of dissociation methods, including treatments with a variety of enzymes, were tested, but with the exception of the heat shock methods described here, none consistently yielded large numbers of pure, intact cnidocytes.

The cnidome of the tentacles of *Physalia physalis* has been reported variously to consist of two size-classes of heterotrichous anisorhizas (Totton and Mackie, 1960), two size classes of spherical isorhizas (Purcell, 1984) and atrichous isorhizas (Weill, 1934). The dissociation procedure employed

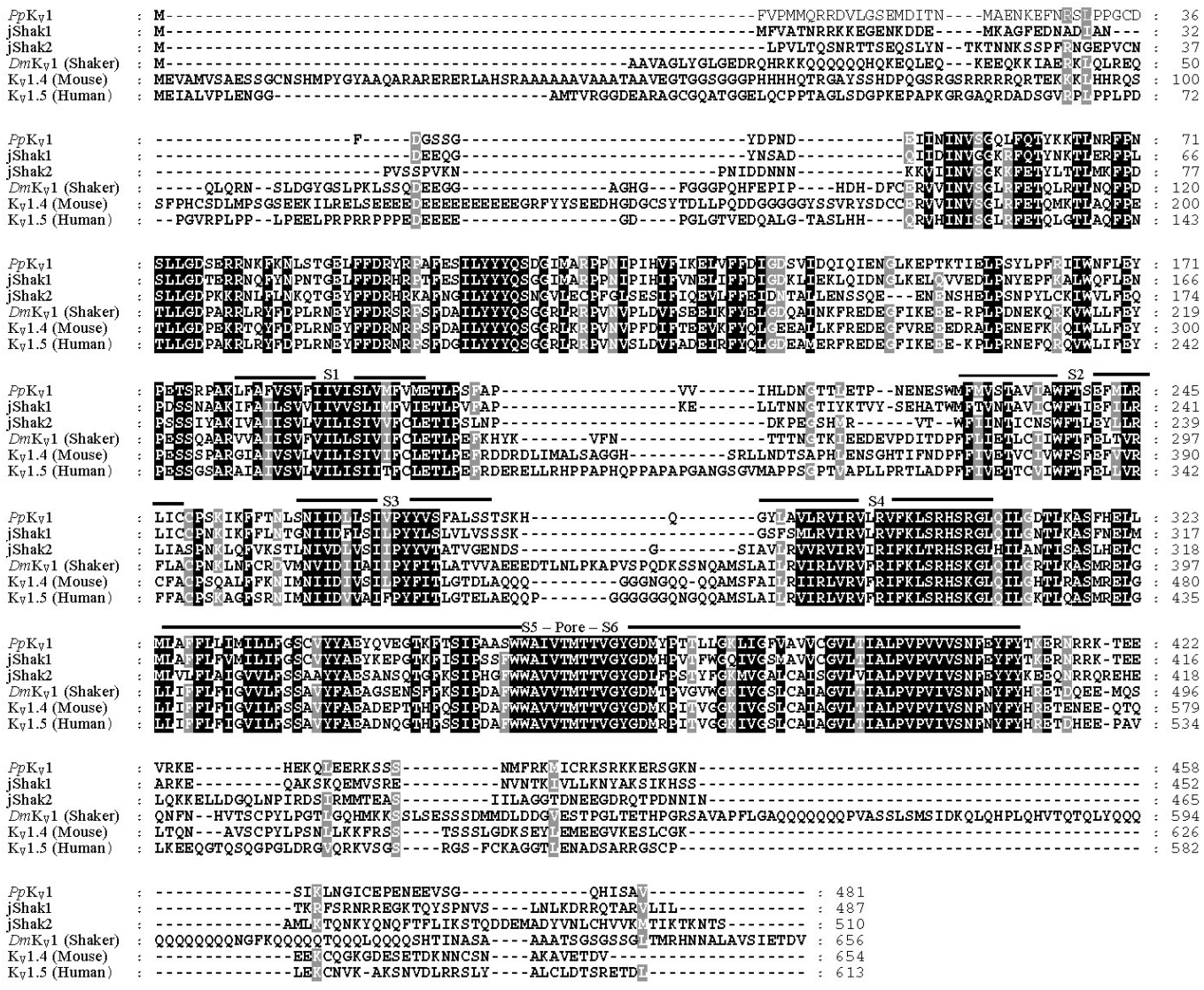

Fig. 5. Alignment of the *Physalia* K^+ channel (GenBank Accession number: ABD59027), with other K_V1 channels including two from jellyfish (jShak1 [Accession number AAB02603] and jShak2 [AAB02604]), the *Drosophila Shaker* channel (*Dm*K_V1 [P08510]), rabbit ($K_V1.4$ [CAB94846]) and human ($K_V1.5$ [NP 002225]). The degree of conservation is indicated as for Fig. 2. The transmembrane segments and pore regions are marked. This alignment was obtained using ClustalX and displayed using Genedoc (Ver. 2.6.002).

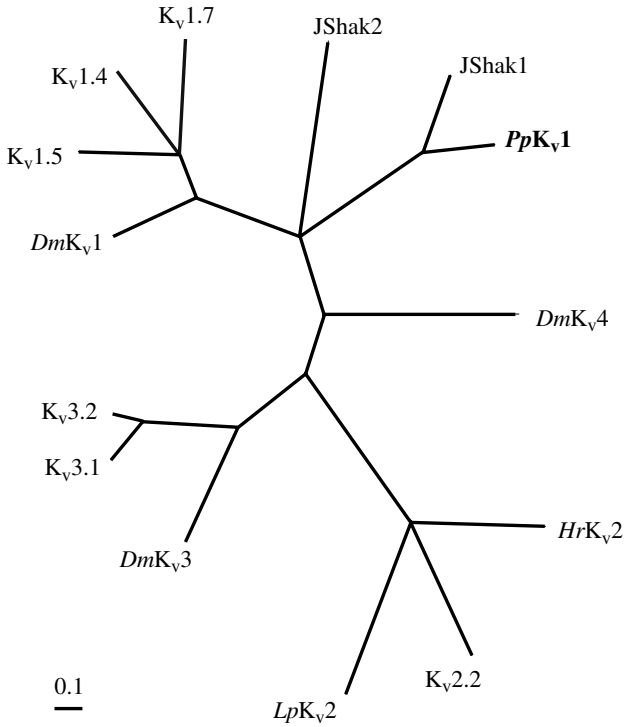

Fig. 6. An unrooted phylogram showing the relationship between *Pp*K$_V$1 (shown in bold type) and other voltage-gated K^+ channels. Channels used in this alignment include jShak1 [AAB02603] and jShak2 [AAB02604] from the hydromedusa *Polyorchis pennicilatus*, the *Shaker* (*Dm*K$_V$1 [P08510]), Shaw (*Dm*K$_V$3 [P17972]) and Shal (*Dm*K$_V$4 [P17971]) channels from *Drosophila*, one each from the squid, *Loligo pealei* (*Lp*K$_V$2 [CAA74748]) and tunicate *Halocynthia roretzi* (*Hr*K$_V$2 [BAA75810], and six mammalian channels, the human K$_V$1.5 [AAH99666] and K$_V$1.7 [NP 114092] channels, the mouse K$_V$1.4 [NP 067250], K$_V$3.1 [NP 032447] and K$_V$3.2 [NP 001020752] channels, and rabbit K$_V$2.2 [Q95L11] channel. Only the bipartitions supported at greater than 95% probability are shown. Scale bar represents the average number of replacements per site.

here yielded large numbers of cnidocytes, of two size classes. The majority of the cells were intact, but the appearance of the few discharged cnidocytes present was consistent with that of the cnidome of *P. utriculus* (Yanagihara et al., 2002), which consists of two size classes of heterotrichous anisorhizas.

The facts that the isolated cnidocytes possess a cnidocil on the apical end of the cell, membrane-bound cytoplasmic extensions at the basal end of the cell, and a DAPI-stained nucleus at the base of the cnidocyst (Fig. 1) were taken as evidence that the isolated, purified cells were intact and, therefore, likely to contain cell-specific mRNA. In the preparations of purified cnidocytes used to prepare the amplified cDNA libraries, the enrichment for cnidocytes was almost total. While occasional loose DAPI-stained nuclei were observed, no other cell types were ever observed. We thus conclude that the cDNA libraries are specific for cnidocytes. Screening these libraries using standard molecular cloning protocols yielded a variety of voltage-gated channel fragments, including *Pp*Ca$_V$β and *Pp*K$_V$1, for which full-length sequences and expression were obtained. Fragments of a Ca^{2+} channel α_1 subunit and a voltage-gated Na^+ channel α subunit, which were isolated using degenerate primers that have isolated Ca^{2+} and Na^+ channel fragments from other cnidarians (Anderson et al., 1993; White et al., 1998; Jeziorski et al., 1998), were not investigated beyond their initial identification.

The Ca^{2+} channel β subunit identified here (*Pp*Ca$_V$β) was isolated using degenerate oligonucleotide primers that have successfully isolated β subunits from another invertebrate. Not unexpectedly, *Pp*Ca$_V$β is phylogenetically closest to *Cy*Ca$_V$β, an equivalent channel isolated from the scyphozoan jellyfish *Cynaea capillata* (Jeziorski et al., 1999), but shows high structural similarity to other β subunits, most notably in the conservation of the residues that interact with the α_1 subunit

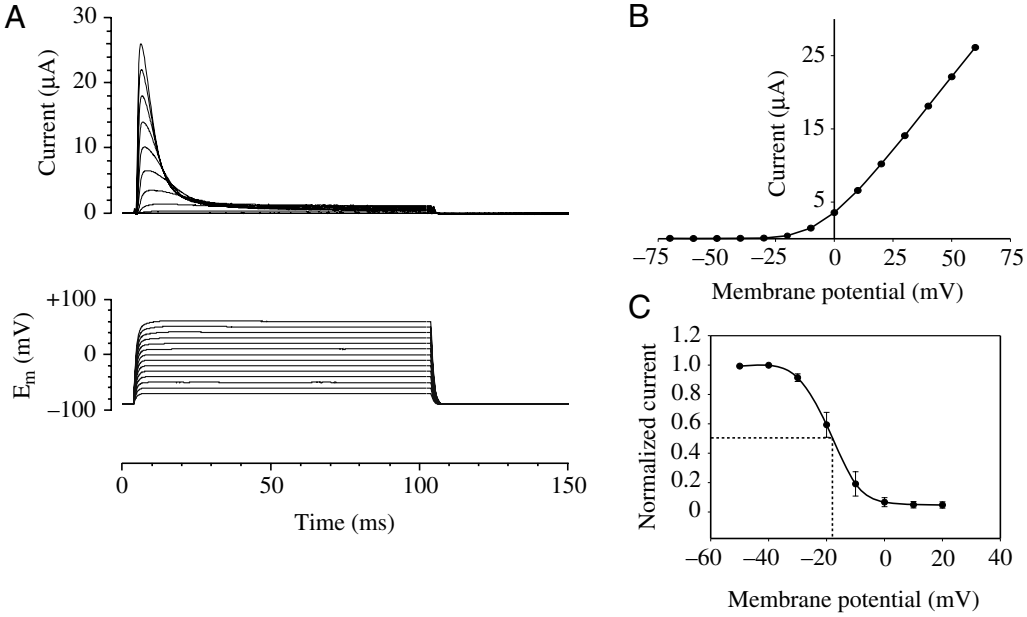

Fig. 7. Functional properties of expressed *Pp*K$_V$1 channels. (A) Family of currents recorded from an oocyte under voltage clamp. (B) Current/voltage relationship of the currents shown in A. (C) An H-infinity plot showing the voltage-dependance of channel inactivation. 50% inactivation occurs at –19 mV.

(Chen et al., 2004; Van Petegem et al., 2004; Richards et al., 2004).

Functionally, *Pp*$Ca_V\beta$ is similar to other β subunits inasmuch as it significantly increases currents through both mammalian ($Ca_V2.3$) and cnidarian (*Cy*Ca_V) Ca^{2+} channel α_1 subunits and, particularly in the case of *Cy*Ca_V, produces a negative shift in the current/voltage relationship of the current. It also increases the time constant of inactivation of currents carried by *Cy*Ca_V. Thus, *Pp*$Ca_V\beta$ is a functional Ca^{2+} β-subunit.

The presence of a voltage-gated K^+ channel of the *Shaker* (K_V1) family in cnidocytes is not surprising. K^+-dependent currents are common in many if not most excitable cells, and K^+-dependent outward currents have been recorded from isolated cnidocytes (Anderson and McKay, 1987). As might be expected, *Pp*K_V1 clusters with other invertebrate members of the *Shaker* (K_V1) family, and is most closely associated with jShak1, a *Shaker*-like channel from another cnidarian (Jegla et al., 1995). The channel contains two consensus sequences for protein kinase A (PKA) phosphorylation (Tyr^{420} and Ser^{437}) located in the C-terminal region. Ser^{437} is highly conserved and corresponds to the site that has been shown to be involved in phosphorylation-dependent modulation of $K_V1.1$ channels (Winklhofer et al., 2003). The functional properties of *Pp*K_V1, including its pharmacology, and the fact that loss of part of the amino terminus of the channel converts it from a fast inactivating channel to a steady-state one, are consistent with the properties of other members of this K^+ channel family (Hoshi et al., 1990).

The discovery that cnidocytes contain Ca^{2+} channels supports the argument that cnidocyte discharge involves voltage-gated Ca^{2+} channels in the cnidocytes, but some caution should be retained. Previous work with cnidocytes in the tentacles of *Physalia* showed that cnidocytes impaled with microelectrodes will not discharge in response to intracellular current injection (Anderson and McKay,1987), implying that discharge does not involve any voltage-dependent phenomena. Furthermore, cnidocytes isolated from the hydroid *Cladonema* have been shown to produce action potentials (Anderson and McKay, 1987; Price and Anderson, 2006), yet neither those action potentials, nor imposed changes in membrane potential, both of which would be expected to activate any endogenous voltage-gated Ca^{2+} channels, trigger discharge. It is, of course, possible that the presence of the microelectrode or the isolation procedure may have compromised the cells' abilities to discharge, but it is also possible that the Ca^{2+} channels reported here may play other roles.

Ultrastructural studies of cnidocytes has revealed the presence of chemical synapses between cnidocytes and other cell types, with the cnidocytes being both presynaptic (Holtmann and Thurm, 2001; Thurm et al., 2004) and postsynaptic (Westfall, 2004). Cnidocytes that provide the presynaptic elements of a chemical synapse would be expected to contain the molecular machinery required for synaptic exocytosis, including a variety of Ca^{2+} channel subunits. Thus, the presence of a $Ca^{2+}\alpha1$ subunit and *Pp*$Ca_V\beta$ in cnidocytes may simply reflect these cells' role as presynaptic elements and should not be unexpected. Confirmation that these channel proteins are involved in cnidocyte discharge will require evidence that these subunits are localized to the apical membrane of the cnidocytes, where cnidocyst exocytosis occurs. Now that the primary structure of these channel subunits has been determined, immunocytochemical localization should be possible.

Supported by NSF grant IBN 0110550. L.S. and M.Z. were supported by the Whitney Laboratory Research Experience for Undergraduates program (NSF grant DBI-9732151). We are very grateful for the assistance provided by Dr M. Matz for the phylogenetic analysis.

References

Aerne, B. L., Stidwell, R. P. and Tardent, P. (1991). Nematocyst discharge in *Hydra* does not require the presence of nerve cells. *J. Exp. Zool.* **258**, 137-141.

Anderson, P. A. V. and McKay, M. C. (1987). The electrophysiology of cnidocytes. *J. Exp. Biol.* **133**, 215-230.

Anderson, P. A. V., Holman, M. A. and Greenberg, R. M. (1993). Deduced amino acid structure of a putative sodium channel from the scyphozoan jellyfish *Cyanea capillata*. *Proc. Natl. Acad. Sci. USA* **90**, 7419-7423.

Anderson, P. A. V., Thompson, L. F. and Moneypenny, C. G. (2004). Evidence for a common pattern of peptidergic innervation of cnidocytes. *Biol. Bull.* **207**, 141-146.

Brinkmann, M., Oliver, D. and Thurm, U. (1995). Interaction of mechano- and chemosensory signals within the same sensory cell. *Pflüg. Archiv. Eur. J. Physiol.* **429**, R153.

Chen, Y., Li, M., Zhang, Y., Yamaha, Y., Fitzmaurice, A., Shen, Y., Zhang, H., Tong, L. and Yang, J. (2004). Structural basis of the α_1-β subunit interactions of voltage-gated Ca^{2+} channels. *Nature* **429**, 675-680.

Chomczynski, P. and Sacchi, N. (1987). Single-step method of RNA isolation by acid guanidinium thiocyanate-phenol-chloroform extraction. *Anal. Biochem.* **162**, 156-159.

Gitter, A. H. and Thurm, U. (1993). Inorganic, but not organic calcium channel blockers inhibit nematocyte discharge in *Hydra vulgaris*. *Eur. J. Cell Biol.* **60** (Suppl. 37), 325-330.

Gitter, A. H., Oliver, D. and Thurm, U. (1994). Calcium- and voltage-dependence of nematocyst discharge in *Hydra vulgaris*. *J. Comp. Physiol. A* **174**, 115-122.

Holtmann, M. and Thurm, U. (2001). Mono- and oligo-vesicular synapses and their connectivity in a cnidarian sensory epithelium (*Coryne tubulosa*). *J. Comp. Neurol.* **432**, 537-549.

Hoshi, T., Zagotta, W. N. and Aldrich, R. W. (1990). Biophysical and molecular mechanisms of Shaker potassium channel inactivation. *Science* **250**, 533-538.

Jegla, T., Grigoriev, N., Gallin, W. J., Salkoff, L. and Spencer, A. N. (1995). Multiple Shaker potassium channels in a primitive metazoa. *J. Neurosci.* **15**, 7989-7999.

Jeziorski, M. C., Greenberg, R. M., Clark, K. S. and Anderson, P. A. V. (1998). Cloning and functional expression of a voltage-gated calcium channel α_1 subunit from jellyfish. *J. Biol. Chem.* **273**, 22792-22799.

Jeziorski, M. C., Greenberg, R. M. and Anderson, P. A. V. (1999). Cloning and expression of a jellyfish calcium channel β subunit reveals functional conservation of the α_1–β interaction. *Receptors Channels* **6**, 375-386.

Kass-Simon, G. and Scappaticci, A. A., Jr (2002). The behavioral and developmental physiology of nematocysts. *Can. J. Zool.* **80**, 1172-1794.

Kass-Simon, G. and Scappaticci, A. A., Jr (2004). Glutamatergic and GABAergic control of the tentacle effector systems of *Hydra vulgaris*. *Hydrobiologia* **530/531**, 67-71.

Kohn, A. B., Anderson Peter, A. V., Roberts-Misterly, J. M. and Greenberg, R. M. (2002). Schistosome calcium channel β subunits. Unusual modulatory effects and potential role in the action of the antischistosomal drug praziquantel. *J. Biol. Chem.* **276**, 36873-36876.

Lingueglia, E., Champigny, G., Lazdunski, M. and Barbry, P. (1995). Cloning of the amiloride-sensitive FMRFamide peptide-gated sodium channel. *Nature* **378**, 730-733.

Lubbock, R., Gupta, B. L. and Hall, T. A. (1981). Novel role of calcium in

exocytosis: mechanism of nematocyst discharge as shown by X-ray micro analysis. *Proc. Natl. Acad. Sci. USA* **78**, 3624-3628.

Lukyanov, K., Diatchenko, L., Chenchik, A., Nanisetti, A., Siebert, P., Usman, N., Matz, M. and Lukyanov, S. (1997). Construction of cDNA libraries from small amounts of total RNA using the suppression PCR effect. *Biochem. Biophys. Res. Commun.* **230**, 285-288.

Matz, M. V. (2002). Amplification of representative cDNA samples from microscopic amounts of invertebrate tissue to search for new genes. *Meth. Mol. Biol*. **183**, 3-18.

Matz, M. V., Alieva, N. O., Chenchik, A. and Lukyanov, S. (2003). Amplification of cDNA ends using PCR suppression effect and step-out PCR. *Meth. Mol. Biol*. **221**, 41-49.

McKay, M. C. and Anderson, P. A. V. (1988). On the preparation and properties of isolated cnidocytes and cnidae. In *The Biology of Cnidocytes* (ed. H. M. Lenhoff and D. A. Hessinger), pp. 273-293. New York: Academic Press.

Page, R. D. M. (1996). TREEVIEW: an application to display phylogenetic trees on personal computers. *Comp. Appl. Biosci.* **12**, 357-358.

Parker, G. H. (1916). The effector systems of actinians. *J. Exp. Zool*. **21**, 461-484.

Price, R. B. and Anderson, P. A. V. (2006). Chemosensory pathways in the capitate tentacles of the hydroid *Cladonema. Invert. Neurosci.* **6**, 23-32.

Purcell, J. E. (1984). The functions of nematocysts in prey capture by epipelagic siphonophore (Coelenterata, Hydrozoa). *Biol. Bull.* **166**, 310-327.

Purcell, J. E. and Anderson, P. A. V. (1995). Electrical responses to water-soluble components of fish mucus recorded from the cnidocytes of a fish predator, *Physalia physalis*. *Mar. Freshw. Behav. Physiol*. **26**, 149-162.

Richards, M. W., Butcher, A. J. and Dolphin, A. C. (2004). Ca^{2+}channel β-subunits: structural insights AID our understanding. *Trends Pharmacol. Sci.* **25**, 626-632.

Ronquist, F. and Huelsenbeck, J. P. (2003). MrBayes 3, Bayesian phylogenetic inference under mixed models. *Bioinformatics* **19**, 1572-1574.

Salleo, A., Musci, G., Barra, P. F. A. and Calabrese, L. (1996). The discharge mechanism of acontial nematocytes involves the release of nitric oxide. *J. Exp. Biol.* **199**, 1261-1267.

Sudhof, T. C. (2004). The synaptic vesicle cycle. *Annu. Rev. Neurosci*. **27**, 509-547.

Thurm, U., Brinkmann, M., Golz, R., Holtmann, M., Oliver, D. and Sieger, T. (2004). Mechanoreception and synaptic transmission of hydrozoan nematocytes. *Hydrobiologia* **530/531**, 97-105.

Totton, A. K. and Mackie, G. O. (1960). Studies on *Physalia physalis. Discov. Rep*. **30**, 301-408.

Van Petegem, F., Clark, K. A., Chatelain, F. C. and Minor, D. L., Jr (2004). Structure of a complex between a voltage-gated calcium channel beta-subunit and an alpha-subunit domain. *Nature* **429**, 671-675.

Watson, G. M. and Roberts, J. (1995). Chemoreceptor-mediated polymerization and depolymerization of actin in hair bundles of sea anemones. *Cell Motil. Cytoskeleton* **30**, 208-220.

Weill, R. (1934). Contributions l'étude des cnidaires et de leurs nématocystes. *Trav. Stat. Zool. Wimereux* **10**, 1-347.

Westfall, J. A. (2004). Neural pathways and innervation of cnidocytes in tentacles of sea anemones. *Hydrobiologia* **530/531**, 117-121.

Westfall, J. A. and Grimmelikhuijzen, C. J. P. (1993). Antho-RFamide immunoreactivity in neuronal synaptic and non-synaptic vesicles of sea anemones. *Biol. Bull*. **185**, 109-114.

White, G. B., Pfahnl, A., Haddock, S., Lamers, S., Greenberg, R. M. and Anderson, P. A. V. (1998). Structure of a putative sodium channel from the sea anemone *Aiptasia pallida*. *Invert. Neurosci*. **3**, 317-326.

Winklhofer, M., Matthias, K., Seifert, G., Stocker, M., Sewing, S., Herget, T., Steinhauser, C. and Saaler-Reinhardt, S. (2003). Analysis of phosphorylation-dependent modulation of $K_V1.1$ potassium channels. *Neuropharmacology* **44**, 829-842.

Yanagihara, A. A., Kuroiwa, M. Y., Oliver, L. M. and Dunkel, D. D. (2002). The ultrastructure of nematocysts from the fishing tentacle of the Hawaiian bluebottle, *Physalia utriculus* (Cnidaria, Hydrozoa, Siphonophora). *Hydrobiologia* **489**, 139-150.